ABSTRACT

CALDERON, VICTOR ALEJANDRO. Condition Dependent Performance Based Design. (Under the direction of Dr. Mervyn Kowalsky.)

Structures located in seismic prone regions are often subjected to multiple earthquakes. Multiple earthquakes can accumulate damage resulting in a deterioration of the seismic performance of a structure. In addition, aging of the structure can arise conditions in the structure such as corrosion that further propagate the deterioration. Past research has shown that the Park and Ang damage index (DI)(a demand parameter that quantifies damage) increases as damage aging conditions in the structures worsen or multiple seismic events are included in the analysis. This increases the probability of a structure to collapse. This research proposes to study the effects of multiple earthquakes and damage accumulation in RC structures by developing strain limit states fragility functions for different aging conditions. To achieve this it is also important to develop limit states that represent corroded reinforcing steel. A method to perform accelerated corrosion in passivated reinforcing steel is proposed. This corroded rebars are then subjected to tension test and buckled bar tension tests, which will later be used to define service limit state and damage control limit state. To show the relevance of this study a framework that incorporates corrosion models into a nonlinear time history analysis (NLTHA) is developed. A series of SDOF cantilever columns are subjected to a sweep of earthquakes. This preliminary results show that there is an increase in the probability of reaching a limit state. The results also show the dispersion of results by using PGA as the impact measure (IM), indicating the need for a better intensity measure. The end results of this research will be to (1) develop fragility curves that consider strain limit states to measure damage while incorporating different aging conditions, (2) establish limit states for corroded rebars, (3) inform the research community on the necessary methodology to accurately model corrosion for material testing and large scale testing of corroded reinforced members (4) consider the effects of multiple earthquakes for main shock sequences and mainshock-aftershock sequence (5) incorporate the results into the direct displacement based design methodology.

Condition Dependent Performance Based Design

by
Victor Alejandro Calderon

A research proposal submitted to the Graduate Faculty of
North Carolina State University
in partial fulfillment of the
requirements for the Degree of
Doctor of Philosophy

Civil Construction and Environmental Engineering

Raleigh, North Carolina

2020

APPROVED BY:

Dr. James Nau	Dr. Mohammad Pour-Ghaz
Dr. Rudolf Seracino	Dr. Thomas Birkland

Dr. Mervyn Kowalsky
Chair of Advisory Committee

TABLE OF CONTENTS

LIST OF TABLES

LIST OF FIGURES

Chapter 1

INTRODUCTION

Structures subjected to multiple events and aging conditions has become an important aspect of Performance Based Earquake Engineering (PBEE).Recent earthquakes sequences such as the Christchurch 2010, Italy Earthquake 1995 and more recently the Puerto Rico Earthquakes 2020, have shown that, structures after sustaining damage during a mainshock have then collapsed or sustained an increased damage after being subjected to a large magnitude aftershock. In spite of these observations, there is not a clear methodology to establish a measure of damage that can represent the effects of cumulative damage on a structure structure. In addition, structures can have an existing condition such as corrosion that furthers deteriorates the structural performance of the structure. Researchers have used the Park and Ang Damage Index (DI) to quantify damage, while this measure has been widely used to study the effects of accumulated damage, this damage index uses calibrated data to specific loading conditions and specific structural systems. Furthermore, the effects of the inelastic have a small effect on the damage index and therefore it does not represent a good estimate of damage. In addition, this damage index and other measures of damage such as drift ratio based limit states have been incorporated into the PEER Performance Based Design Probabilistic Framework. While the research shows agreement to the fact that there is an increase in the probability of damage or even collapse of a structure due to repeated loading or increasing the aging conditions, such as high corrosion levels (CL), these results are not based on a tangible measure such as well established strain based limit states.

Therefore, it is the purpose of this research to consider the effects of cumulative damage in the seismic performance of RC structures. Specific aging conditions of interest include corrosion, strain aging, low cycle fatigue and strength aging. Moreover, there is a high likelihood for a structure in a high seismic region to be subjected to more than one main shock throughout

its life, thus, it is deemed important to consider the effects of multiple earthquakes. One of the aging conditions that more significantly deteriorates the seismic response of a structure is corrosion, thus it is important to determine the limit states of corroded reinforcing steel. To determine these limit states a series of material tests will be implemented for this research. Also, an analytical procedure is implemented such that it considers the effect of aging conditions on structures. In specific, this study starts by evaluating a cantilever RC bridge Column. A series of condition dependent nonlinear time history analysis are performed assuming that a series of earthquakes occurs throughout the lifetime of the structure while at the same time changing the properties of the structure as time progresses. At the end of each series the main variables of study are the limit state that was reached, the controlling mode of response (flexural or shear controlled), Equivalent Viscous Damping and the accumulated deformations. The series of earthquake proposed consists of (1) equally spaced main shocks only, (2) main shock-aftershocks series. This research will show how the effects of different aging conditions on the performance of a structures, establish strain limit states as a measure of damage, determine the effect of corrosion in establishing limit states, define what are the effects of multiple earthquake in the functionality of a structure and incorporate results into the Direct Displacement Based Design (DDBD) methodology.

1.1 Scope and layout

This research proposal describes the main components and objectives for the graduate studies of the author of this document. Chapter 2 contains the literature review which summarizes the state of the art in damage measurements and performance based design framework. Chapter 3 covers the research gap and objectives. Chapter 4 summarizes the experimental and analytical procedures relevant to this study. Chapter 5 details the processing of current results.

Chapter 2

LITERATURE REVIEW

Bridges are designed based on discrete events with minimal consideration of interactions between hazards/loading, material aging condition and bridge performance. The purpose of the research described is to study Condition Dependent Performance Based Design that considers the effects of cumulative damage in structures in seismic prone regions.

In this chapter the available knowledge on the different topics that are available in the literature are synthesized. First a review on the different definitions of commutative damage is presented then the main idea for this research are established and the required components, then the different elements that form part of this study are presented and a general concept is established and presented in Chapter 3.

2.1 Cumulative Damage

There have been attempts by many researchers to establish the best way to account for the accumulation of damage.

2.1.1 Damage Index

The effect of commulative damage in structures was first studied by by Park and Ang (1985) [37] in their study the authors proposed the Damage Index as shown in 2.1. The damage index was used as a measure to quantify damage in terms of the maximum experienced earthquake and the absorbed hysteretic energy.

$$D = \frac{\Delta_m}{\Delta_u} - \beta \frac{E_h}{F_y \Delta u} \tag{2.1}$$

Δ_m: Maximum deformation under earthquake
Δ_u: Ultimate deformation under monotonic loading
F_y: Calculated yield strength
E_h: Total hysteretic energy
β: Dimensionless constant

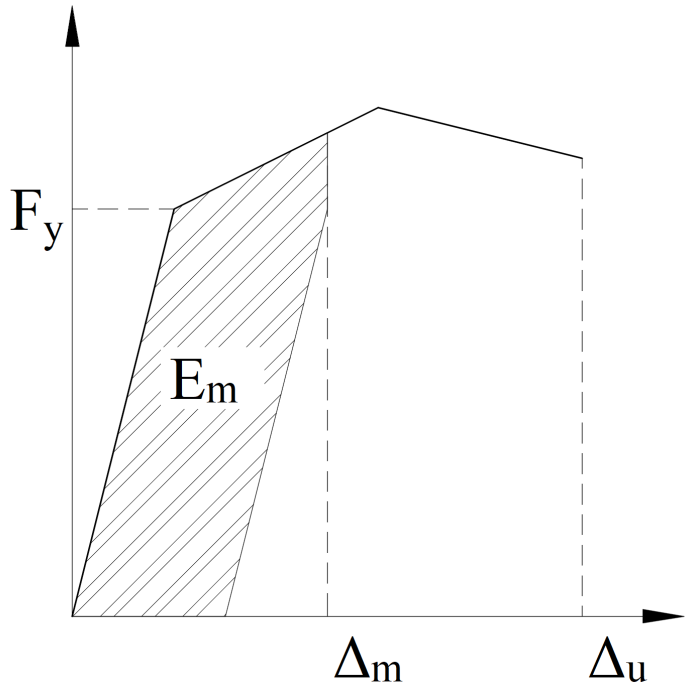

Figure 2.1 Park and Ang conceptual scheme

Equation 2.1 was derived for concrete elements. The first term here is a simple, pseudo-static displacement measure. The second term accounts for cumulative damage. A figure on the concept is shown in Fig. 2.1. The advantages of this model are its simplicity, and the flexibility on adpating the model to correlate with experimental data.

This model has several limitations. Firstly the calibration of the β coefficient with observed damage, has shown to be very low ($\beta = 0.05 - 0.15$) [37] [12], rendering the second term relatively inconsequential compared to the contribution of the first term. A sample result taken from [12], this study used a modified version of the Parnk and Ang damage index in terms of

moment, rotation (θ_y) and curvature ductility (μ).

$$D = \frac{\mu_m}{\mu_u} - \beta \frac{E_h}{M_y \theta_y \mu u} \tag{2.2}$$

using values: $\mu_m = 4.93$; $\mu_u = 17.02$; $M_y = 8751.375$; $\theta_y = 0.0042$; $E_h = 119.07$; $\beta = 0.05$ substituting in the equation:

$$D = \frac{\mu_m}{\mu_u} - \beta \frac{E_h}{M_y \theta_y \mu u} = 0.3 \tag{2.3}$$

First term

$$\frac{\mu_m}{\mu_u} = \frac{4.93}{17.02} = 0.2897 \tag{2.4}$$

Second term

$$\beta \frac{E_h}{M_y \theta_y \mu u} = 0.05 \frac{119.07}{8751.375 * 0.0042 * 17.02} = 0.0103 \tag{2.5}$$

It can be seen that 97% of the damage index comes from the first term which is the elastic term and the inelastic part is only 3% of the total. In addition, the model was derived for reinforced concrete with poor shear detailing. The correlations observed in this model also showed the data to be sparse.

Depite its limitation, several studies have used or modified this model to study the effects of cumulative damage for different structures, of relevant importance are those performed by [18], who used a modified Park and Ang model, to model damagae at the local level for elements in a structural analysis program IDARC 3.0, in this software for the case of multiple degrees of freedom buildings they also added parameters to consider the damage at the inter-story level and the global model. Ghosh et al [12] developed a damage accumulation framework to develop probabilistic estimates of exceeding a damage index for multiple ground motions. Other regressions have been proposed by [15], [8], [29] but show no improvement in assessing the damage state of a structure. While these studies provide an insight into some of the characteristics of damage accumulation they rely on the Park and Ang model and therefore carry the same limitations.

Krawinkler (1987) [16] proposed a method that would consider damage as a function of low cycle fatigue parameters, the form of this damage index for steel component, weldements and local buckling have a general shape of the Miner model. This model relies on the accumulation of plastic deformations. While this model has proven to work well for the evaluation of individual

elements it does not provide a way to generalize damage for other types of structures.

2.1.2 Probabilistic Approach

Increasing interest on the effect of cumulative damage has been experienced over recent years. These studies have focused on determining what is the increase in the risk of a structure due to the accumulation of factors due to many reasons such as multiple earthquakes, corrosion and life span of the structure. Two main approaches have been observed:

- Probabilistic Framework
- Fragility Curves

Proabilistic network

One of the most widely used probabilistic network is the Pacific Earthquake Engineering Research Center (PEER) Performance Based Design. PEER PBD can be expressed by the following equation:

$$\nu_{DM}(dm^{LS}) = \iint D_{DM|EDP}(dm|edp)|, dG_{EDP|IM}(edp|im)||\, d\nu_{IM}(im)| \tag{2.6}$$

Mackie et al [20] on the basis of the PEER PBD developed the Performance Based Damage Design (PBDD) and Perfomance Based Loss Design (PBLD) by defining the probabilistic demand, damage, and loss model parameters in terms of reinforced concrete column damage. The RC column damage was defined on terms of drift ratios defined for the limit states of concrete spalling, bar buckling and failure.

The authors show that for a given intensity measure (IM) and a confidence level of achieving a limit state, its is possible then to define the probability of exceeding that limit state.

While this methodology was able to define damage and incorporate it into the PEER PBD framework, the authors did not consider strain to define the limit states. Also recent research has shown that other intensity measures such as spectral displacement at effective first mode period provide a better intensity measure [17].

Fragility Curves

Another common trend in this subject is the use of fragility curves to estimate the effect of damage in structures. Two main approaches were found in the literature one of them relied on the Park and Ang Model Damage Index to define damage. The second approach relates damage to drift.

Ghosh et al [12] formulated a damage acumulation framework. This study relied on the Park and Ang Damage index explained in the previous section. The study performed a series of nonlinear time history analyses for two cases:

- Using a constant main shock hazard occurrence rate (3 main shocks in a 50 year period)
- Mainshock - Aftershock series using time-dependent aftershock hazard occurrence rate

Evaluation of the damage index exceedance probability for the two cases was performed. The results from this study show regression equations that statistically predict the damage index as a function of earthquake intensity and damage history. This study revealed that for both main shock and aftershock scenarios there was a significant increase in the probability of damage index exceedance under repeated shock scenarios. While this study shows the importance of considering damage accumulation, these results have to be taken with caution since it carries the same disadvantages of the Park and Ang damage index.

Ghosh et al [11] also studied the effects of corrosion in time dependent seismic fragility curves. This study characterizes corrosion in concrete columns as a continuous phenomena that occurs as a function of time. Additionally the authors considered the effects of corrosion in steel bridge bearings. The authors then ran a series of NLTHA analysis for different aging times of the structures. Based on those analysis time dependent fragility curves were presented. The results showed that as time increases, and as a consequence corrosion increases, the probability of exceeding a limit state increases. In this study limit states where defined on the basis of inter-story drifts which were obtained from experimental results and field observations [26]. It is important to mention that limit states were not defined on the basis of strains or other structural property rather from a survey performed in central southeastern United States departments of transportation on the premise of a range of experienced inter-story drifts and the time to repair them. Additionally assuming that corrosion is a continuous process has to be cautiously taken as valid since this is seldom the case in real structures.

While these studies provide a general view on how damage increases the likelihood of observing collapse or deterioration of the seismic performance, the methods used to arrive to those conclusions can be misleading since the definition of damage as either a Damage Index or Drift are not the best parameters to quantify damage. It is our belief that strain based limit states will provide a better understanding and implications on the damage accumulation.

Chapter 3

Study Gap

3.1 Research Gap

It is clear that while studies have tried to show the importance of damage and multiple shocks through the lifetime of a structure, it is important to develop a model that helps to better represents the damage and the earthquake hazard within the performance based design procedure. As structures in the United States continue to age and advances in the earthquake engineering community continue, it is important to provide, accurate estimates of damage, as well as the impacts of aging conditions in bridges seismic performance. In addition, a structure can be subjected to more than a single mainshock and its corresponding aftershocks during the life of the structure.

Damage accumulation is topic that has been gaining momentum in the engineering community since these efforts will better inform what are the potential damages that structure can observe to stakeholders such as state DOTs, building owners and practicing engineers. Damage accumulation has been studied using the Park and Ang damage index or drift based limit states to measure damage accumulation. Different researchers have also included corrosion into their scope of analysis, which shows that aging conditions play an important role in the deterioration of a structure. In addition the literature uses the peak ground acceleration (PGA) as the controlling intensity measure (IM). This research will develop a parametric study using a series of single degree of freedom (SDOF) systems and subjecting them to different conditions such as corrosion, steel strain aging and strength aging among other. The SDOF structures will be subjected to a sweep of ground motions using nonlinear time history analysis to obtain maximum strain demands. With the results obtained fragility functions wo;; ne proposed for each limit state and aging condition. This research will provide the engineering

community with a framework to account for damage in their analysis and guide decisions on the resiliency of a structure. In addition, this study will provide a methodology in which the Direct Displacement-Based Design (DDBD) is modified to consider the effects of damage and conditions.

3.2 General Objectives

The main goal of this research is to provide a methodology to consider damage into the PEER performance based design and demonstrate the implications of aging conditions and multiple earthquakes in the probability of collapse of a structure.

3.3 Specific Objectives

- Incorporate different existing conditions and Develop fragility curves that considers strain limit states as a measure of damage
- Establish limit states for corroded rebars
- Inform the research community on necessary methodology to model corrosion for material testing and large scale testing
- Consider the effects of multiple earthquakes for two cases: (1) Mainshock sequences (2) Mainshock-Aftershock sequence
- Incorporate results into the Direct Displacement Based Design (DDBD) methodology

Chapter 4

Methodology

A methodology that incorporates the different sources of cumulative damage in RC structures is proposed. Different analytical models for aging conditions are studied, this are then incorporated into the analytical model.

The aging conditions focused on this paper are:

- Corrosion
- Strain aging

Other aging conditions will be added to this study.

4.1 Corrosion

One of the main phenomenon that affect the long term behavior of RC structures is corrosion of the reinforcing steel. Two types of corrosion are possible:

- Carbonation,
- Chloride attack

The main source of corrosion in most RC structures is **Chloride Attack**, therefore used in this research.

Corrosion of steel in concrete is an electrochemical process [24] this corrosion may be generated in two ways:

- Composition cells may be formed when to dissimilar metals are embedded in concrete or when significant variations exist in the surface characteristics of steel

- In the vicinity of steel concentration cells may be formed due to differences in the concentration of dissolved ions, such as alkalies and **chlorides**.

The corrosion process of reinforced concrete structures under chloride attack consists in the loss of the protective film on the reinforcing steel surface, this process is known as **depassivation**, after which the initiation of corrosion occurs, the electrical resistivity and the oxygen content control corrosion. Figure 4.1 schematically show this process.

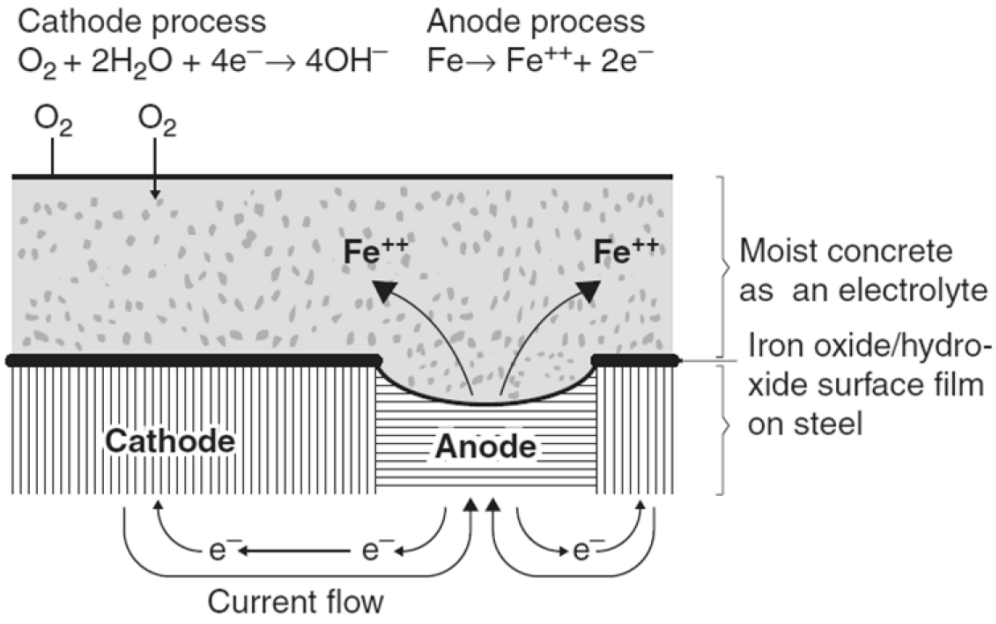

Figure 4.1 Corrosion Process in Reinforcing Steel Bar [24]

Since corrosion plays an important role in the further deterioration of the seismic response of a structure, the following topics have been studied and later incoprorated in the analysis:

1. Time to Initiation of Corrosion (Tcorr)
2. Corrosion growth in reinforcing steel
3. Mechanical Properties of Corroded Reinforcing Steel
4. Cyclic Test on Corroded RC Columns

4.1.1 Time to corrosion

Time to corrosion refers to the corrosion initiation at which the passive film of the reinforcing steel is destroyed and reinforcement starts corroding actively. It has been established that reinforcing steel corrosion follows Fick's law of diffusion [11][32][31][35]. Fick's law is used to model the rate of chloride penetration into concrete as a function of concrete cover and time.

$$\frac{\partial C(x,t)}{\partial t} = D_c \frac{\partial C(x,t)}{\partial x^2} \tag{4.1}$$

$C(x,t)$: Chloride ion concentration x: Distance from concrete surface t: Time in seconds of exposure to chloride ions D_c: Chloride diffusion coefficient

After solving equation 4.1 the following expression for chloride ion concentration results:

$$C_(x,t) = c_0 \left[1 - erf^{-1}\left(\frac{x}{2\sqrt[2]{D_c t}}\right)\right] \tag{4.2}$$

In equation Eq. 4.2 considering a critical chloride corrosion threshold C_r , and a equilibrium chloride concentration C_0 and solve for t, the time to corrosion can be calculated as [11]:

$$T_{corr} = \frac{x^2}{4D_c}\left[erf^{-1}\left(\frac{C_0 - C_{cr}}{C_0}\right)\right]^{-2} \tag{4.3}$$

D_c: Diffusion Coefficient
C_0: Equilibrium Chloride Concentration
C_r: Critical Chloride Concentration

Mean values for C_0 and C_r have been previously defined by many researchers [11][34][7]. These values have been determined for environments that are controlled by **dicing salts**. The values of initiation of corrosion using this values would provide mean times to corrosion in the United States, however this values can be obtained for specific sites if desired.

4.1.2 Rate of corrosion

To estimate the loss of steel cross section due to corrosion a time dependent corrosion rate model been developed [33][31], this model implies that corrosion rate decreases with time. As corrosion accumulates around the reinforcing steel, the corrosion byproducts prevent the uncorroded steel

to react with the environment. The model is shown in Eq. 4.4. This model establishes that the corrosion rate is a function of the water to cement ratio (w/c) and the cover depth (d_c).

$$i_{corr} = \frac{37.5(1 - w/c)}{d_c} \tag{4.4}$$

In Fig. 4.2 the behavior of this model for different values of w/c ratios is shown. It can be seen that at larger values of cover depth the rate of corrosion decreases rapidly and as the water cement ratio increases the rate of corrosion decreases.

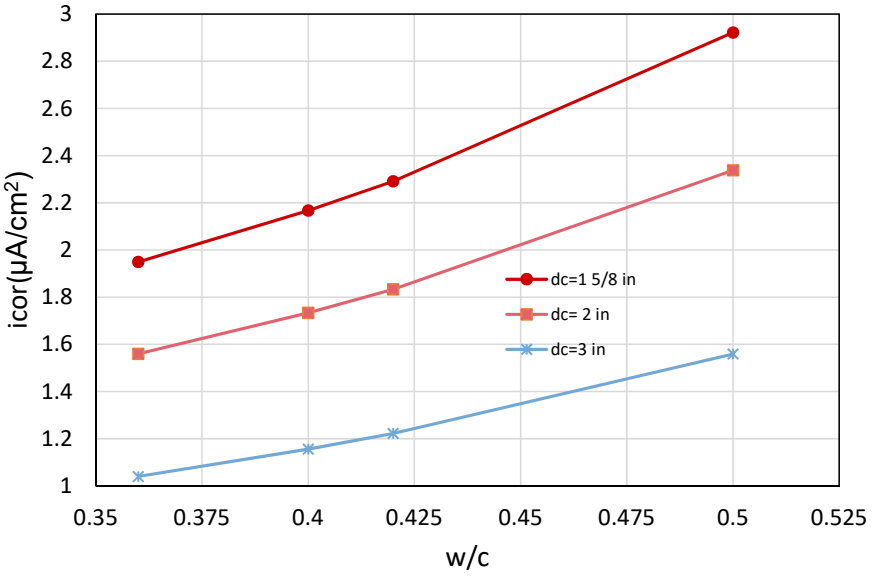

Figure 4.2 Concrete ater to cement ratio vs rate of corrosion

With the rate of corrosion clearly stated, the evolution of corrosion of reinforcement can be calculated. Many researchers have used the model proposed by Vu et al [31][33][5][11] shown in equation Eq. 4.5 and a grpahical representation of the evolution of corrosion for a reinforcing steel of diameter 3/4 inch is for different water to cement ratios is shown in Fig. 4.3

$$d_{corr}(t) = d_{bi} - \frac{1.0508(1 - w/c)}{d_c}(t - t_{corr})^{0.71} \tag{4.5}$$

d_{bi}:Initial diameter of the bar (mm)

The evolution of corrosion in reinforcing steel can be expressed in the percent loss of mass

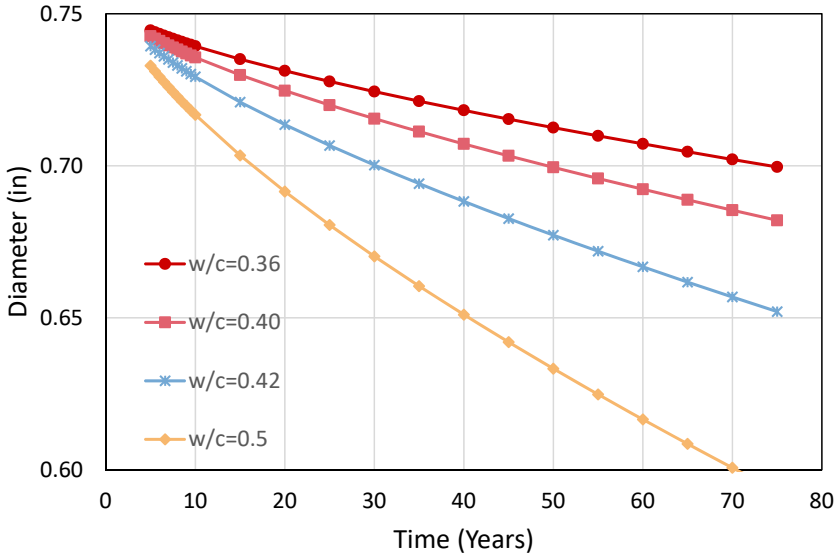

Figure 4.3 Diameter decrease due to corrosion

of a rebar. Since uniform corrosion is assumed this can be expressed in terms of the change in diameter. This is calculated in Eq. 4.6.

$$CL = \frac{d_i - d(t)}{d_i} * 100 \tag{4.6}$$

The values obtained from Eq. 4.5 can then be used in Eq. 4.6 to obtain the variation of Corrosion level as a fuction of time, shown in Fig. 4.4.

4.1.3 Corrosion modified properties of reinforcing steel bars

In a study presented by Yuan et al [38] it was shown from experimental results that the mechanical properties of steel cahnge with the level of corrosion. An expression that shows the variation of yield strength and ultimate strength were provided as follow:

$$f_{y,C} = f_{yo}(1 - 0.021C) \tag{4.7}$$

$$f_{u,C} = f_{yo}(1.018 - 0.019C)$$

$$\delta_{s,C} = \delta_{so}(1 - 0.021C)$$

$$\varepsilon_{y,C} = \varepsilon_{yo}(1 - 0.021C)$$

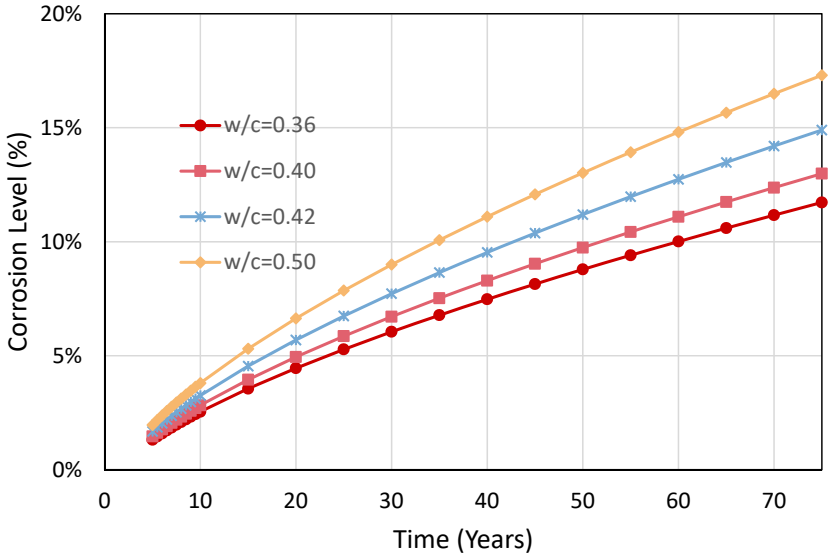

Figure 4.4 Corrosion Level vs Time (years)

These expressions are used in the analytical procedure and as shown in Chapter 5, they correlate well with the observed experimental work.

4.1.4 Physical test on corroded RC Structures

Recent studies [19], [23] and [36] have been developed to assess the force-displacement relationships in cantilever RC Columns. These columns were subjected to Quasi-Static Loading Protocol. These concrete columns were subjected to accelerated corrosion to obtain different Corrosion Levels (CL), the range of CL for these studies correspond to $CL = 0\%20\%$. In these studies the accelerated corrosion was performed via an electrochemical process directly applied to the reinforcing steel as shown in Fig. 4.5.

The resulting force displacement of these experiments is shown in Fig. 4.6 it can be seen that there is a reduction not only on the strength of the system but also on the displacement capacity.

As stated in the previous section the mechanical properties of steel are affected by corrosion. In the previous studies [23] the authors performed tension tests on corroded reinforcing steel. In these tests a reduction in the mechanical properties of steel was observed as well as a reduction in the rupture strain ε_{srup}, see Fig. 4.7.

While these studies show how corroded RC Columns behave under cyclic loading, they did

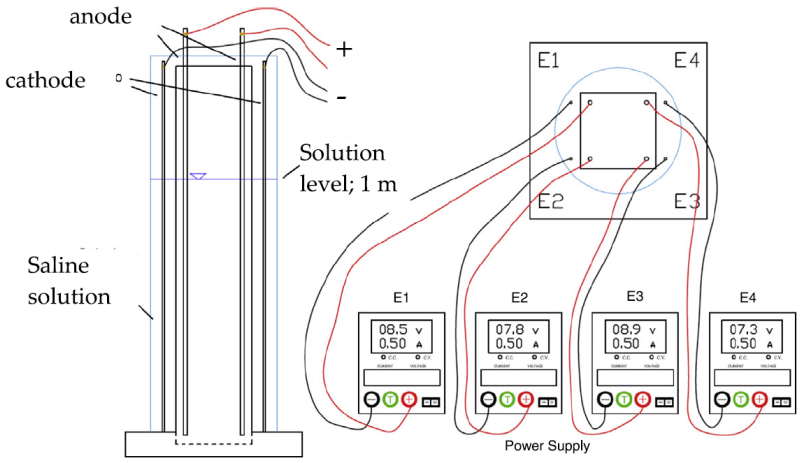

Figure 4.5 Force displacement response of RC Corroded Columns [23]

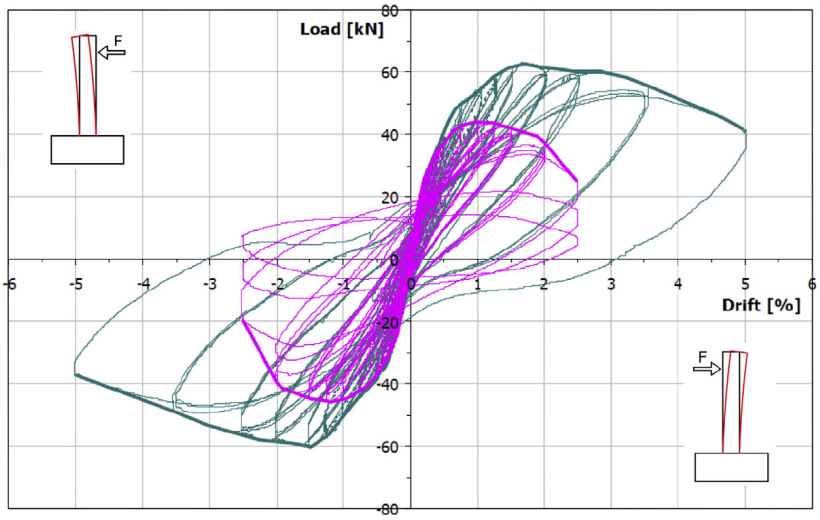

Figure 4.6 Corrosion Process for RC Column [23]

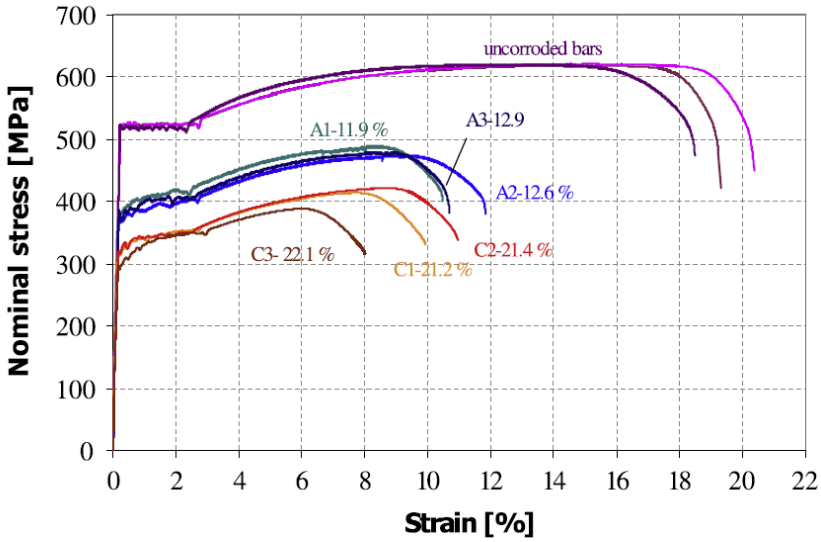

Figure 4.7 Corroded Rebars Stress-Strain Curves [23]

not considered the generation of the protective film due to the alkaline environment of the concrete, this film can modify mechanical properties of corroded steel. Additionally the accelerated corrosion process used a 3% $NaCl$ concentration solution while the chloride attack in concrete usually has a 1.0% - 1.5% concentration of the same Chloride. Therefore the results obtained from these studies do not accurately represent the actual conditions of corroded RC columns. Therefore an experimental campaign is proposed that will provide results on the mechanical behavior of corroded reinforcing steel inside concrete. This is discussed in the following subsection.

4.1.5 Proposed Experimental campaign

As explained in the previous section the steel inside concrete generates a protective film and after chloride attack reaches the surface of the steel, this protective film starts to be eliminated. This same process will be simulated through the an experimental campaign outlined here:

1. Passivation of reinforcing steel
2. Accelerated corrosion of Reinforcing Steel
3. Tension Tests
4. Buckled Bar Tension (BBT) Test

Passivation of reinforcing steel

Methods to generate the passive film on reinforcing steel are available in the literature [10]. According to this study it is possible to generate the passivation process in the same way as it occurs to reinforcing steel inside the concrete. A porous solution will be generated with the following chemical components that are present inside the cement paste:

- Saturated Calcium Hydroxide $Ca(OH)_2$
- Sodium Hydroxide $Na(OH)$ 4.00 g/l
- Potassium Hydroxide (OH) 11.22 g/l
- Calcium Sulfate Dihydrate $Ca(SO)_4 + 2H_2O$ 13.77 g/l

The rebars will be placed in a container with the pore solution for a minimum of 8 days. Annodic Polarization Tests will be measured on the rebars to determine the passive current density. A figure of this process is shown in Fig. 4.8. Additionally The ends of the rebars will be protected to prevent corrosion in these zones of the specimens, the protection at the ends is based from the standard ASTM G109-07 with some alterations. Figures Fig. 4.9 and Fig. 4.10 show the specimen geometry and the preparation of the ends of the rebars.

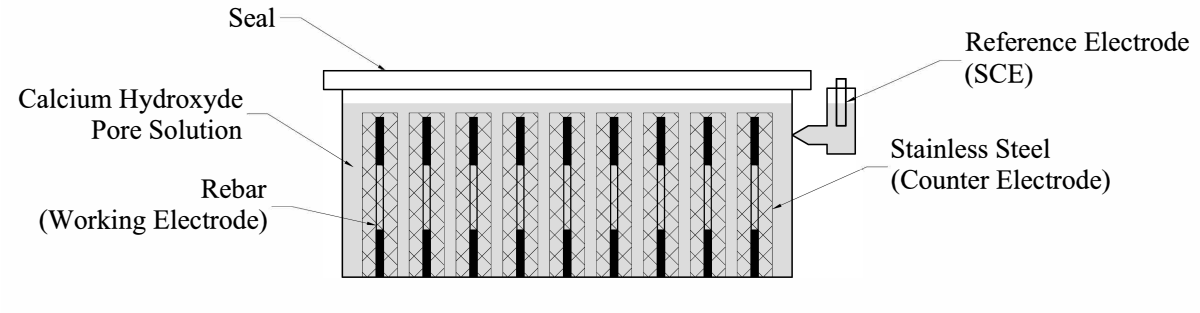

Figure 4.8 Rebars Passivation Process in Calcium Hydroxyde Pore Solution

Accelerated corrosion of Reinforcing Steel

The accelerated corrosion will be done by using a galvanic cell. Different studies [10] has shown that for rebars with pasive films a concentration of 0.3 Moles of sodium chloride $(NaCl)$ will start the depassivation process on the rebars. The rebars will be subjected to a current of

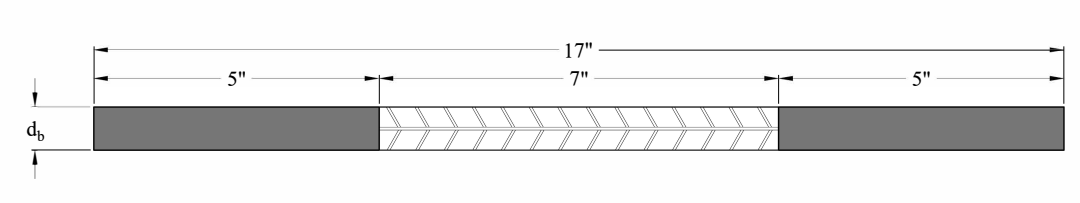

Figure 4.9 Rebar Specimen Geometry

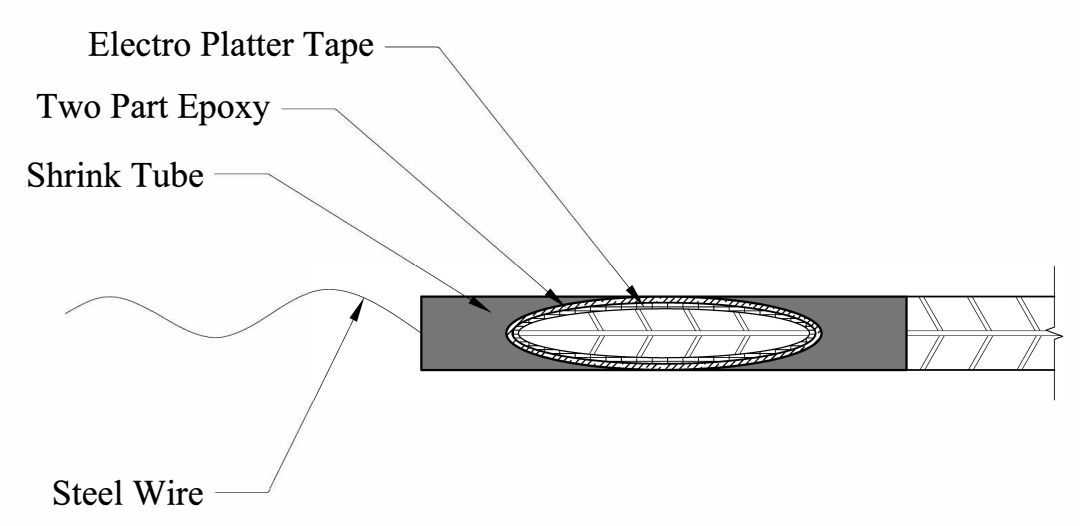

Figure 4.10 Rebars Ends Protection

. This current is sustained for a period of time according to Faraday's Law until the desired level of corrosion is reached:

$$t = \frac{\lambda m_{loss} \eta_{specimen} C_{faraday}}{i M_{specimen}} \tag{4.8}$$

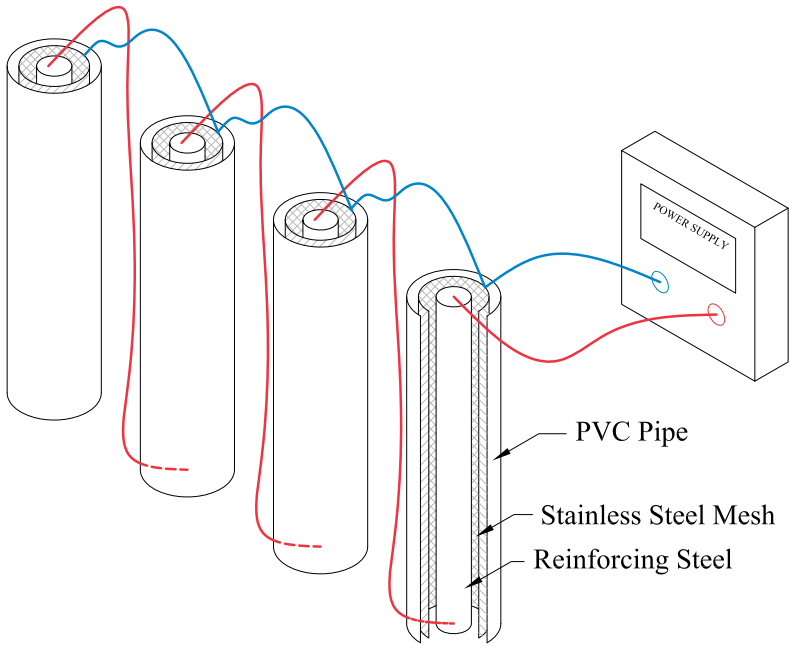

Figure 4.11 Accelerated Corrosion Process

For the different rebar sizes and Corrosion levels the current and the Time of Application is shown in Table 4.1. A current of $5mA$ is applied to the specimen obtaining the time this current needs to be applied for.

Tension Tests

A series of ension tests will be performed according to ASTM A706. The main objective of this tests is to evaluate differences in the Stress-Strain behavior of corroded Reinforcing Steel. This will help in determining any reduction in the ductility of steel for this condition. In addition equations 4.7 will be corroborated.

Table 4.1 Accelerated Corrosion to achieve Corrosion Levels.

Corrosion Level (CL)	Mass loss (g)	time(days)
5%	1.12	9
10%	2.24	18
15%	3.36	27
20%	4.47	36
25%	5.59	45

Buckled Bar Tension (BBT) Test

One of the limit states that control Performance Based Design is Buckling of Reinforcing steel, recent tests have been developed to determine the critical bending strain of buckling of reinforced steel [3]. The premise of the BBT Test is a material test to simulate bending and tension strain demands on a buckled bar.However those results have been developed for rebars in pristine condition, it is therefore necessary to check if available expressions to determine this limit state hold for corroded steel.

The Buckled Bar Tension Test consists in:

1. Compress a rebar specimen up to a certain level of compression strain such that the rebar will show buckling
2. The rebar is then pulled untill rupture
3. process is repeated for different levels of compression strains

This test is proposed for different levels of corrosion such that any changes on the behavior are studied and incorporated into the analysis a sequence of the test procedure is shown in Fig. 4.12. A proposed test matrix is shown in Table 4.2.

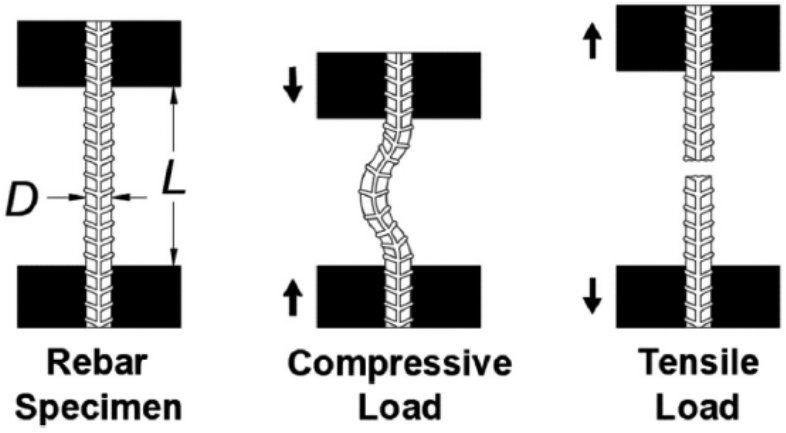

Figure 4.12 BBT Test sequence

Table 4.2 Corroded Rebar Test Matrix

Corroded BBT Test Matrix			
Test	Diameter of Bar	CL (%)	Number of Tests
Tension Test	#6	0	3
		5	3
		10	3
		15	3
		20	3
		25	3
BBT Test	#6	0	6
		5	6
		10	6
		15	6
		20	6
		25	6

4.1.6 Modeling of corrosion for Structural Analysis

The previous elements of corrosion explained in the previous sections are incorporated into the structural analysis mainly at the material level. The application can be outlined as follows:

1. First the time for initiation of corrosion is calculated according to the Gosh and Padgett Model [11]
2. Then the rate of corrosion is calculated according to the Vu et al model [33]
3. Following this the size of the rebar is reduced and the corrosion level is calculated
4. Finally the mechanical properties of the reinforcing steel are modified with the corresponding corrosion level.

This modeling can be better seen in Fig. 4.13

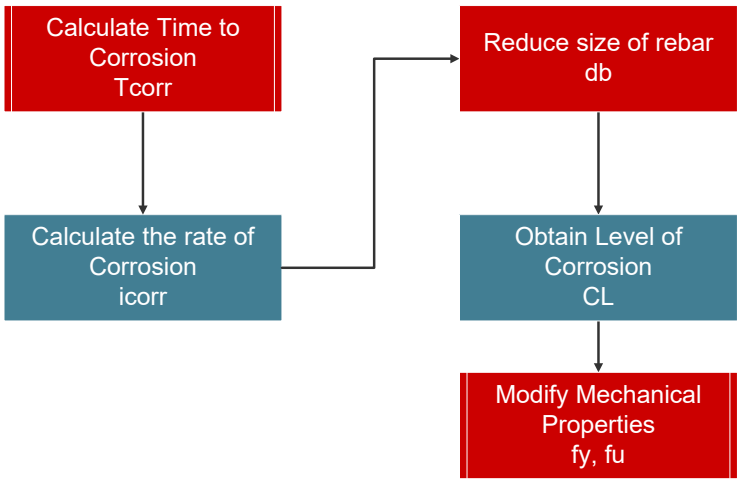

Figure 4.13 Corrosion Modeling for Structural Analysis

This is later incorporated into the Nonlinear Structural Analysis Framework using the package OpenSees [22], the framework of this analysis is explained in [**Chapter-5**].

4.2 Steel Strain Aging

4.2.1 Metallurgical Process

It is generally accepted that strain aging is due to the diffusion of carbon and/or nitrogen atoms in solution to dislocations that have been generated by plastic deformation. Initially, an atmosphere of carbon and nitrogen atoms is formed along the length of a dislocation, immobilizing it. Extended aging, however, results in sufficient carbon and nitrogen atoms for precipitates to form along the length of the dislocation.

These precipitates impede the motion of subsequent dislocations, and result in some hardening and loss in ductility. The extent of strain aging, which is a thermally activated process, depends primarily on aging time and temperature. In general, extended aging results in a saturation value above which further aging has no effect.

A second strengthening mechanism occurs when cold deformation (alone) is applied to steels. When dislocations break away for their pinning interstitial atoms and begin the movement causing slip they begin to intersect with each other. A complex series of interactions between the dislocations occurs, causing them to pin each other, decreasing their mobility. The decreased mobility also results in higher strength, lower ductility and lower toughness. As a result, cold deformed steels already have lowered ductility and toughness before any strain aging occurs and when heating follows cold deformation, the loss in ductility and toughness is greater. It is this combination of events that is the most damaging to the toughness of structural steels.

4.2.2 Strain aging effects in structures

Since it has already been established that strain aging is the process in which steel after being subjected to large strains develops an increased strength and reduced ductility with time and therefore important to include it in a time dependent analysis, considering the fact that plastic hinges will form in a ductile structure and the steel could reach high strains in this regions of the structure. Furthermore strain aging will cause an increased in the strength of the plastic hinge and as a consequence plastic hinges might be formed in regions of the structures that have not been designed for such demands. The effects of strain aging may also alter the transverse reinforcement due to both cold bending, making them susceptible to brittle failure.

According to [28] most strain aging occurs in the first 37 days. Also [25] studied strain aging effects with respect to time for different levels of pre-strains that ranged from $2\varepsilon_y - 10\varepsilon_y$ and for a time frame of 3 days to 50 days, from this study it was determined that a significant effect of strain aging took place from pre-strains $5\varepsilon_y$ and on. Strains higher than $15\varepsilon_y$ indicate

a performance level in which substantial damage has been induced in the structure such that it is deemed unrepairable and therefore pre-strains higher that $15\varepsilon_y$ are unpractical and not studied by Montahan et al[25].

Momtahan et al was able to correlate the increase in yield strength as a function of time and the pre-strain in reinforcing steel bars. The proposed equations are shown below:

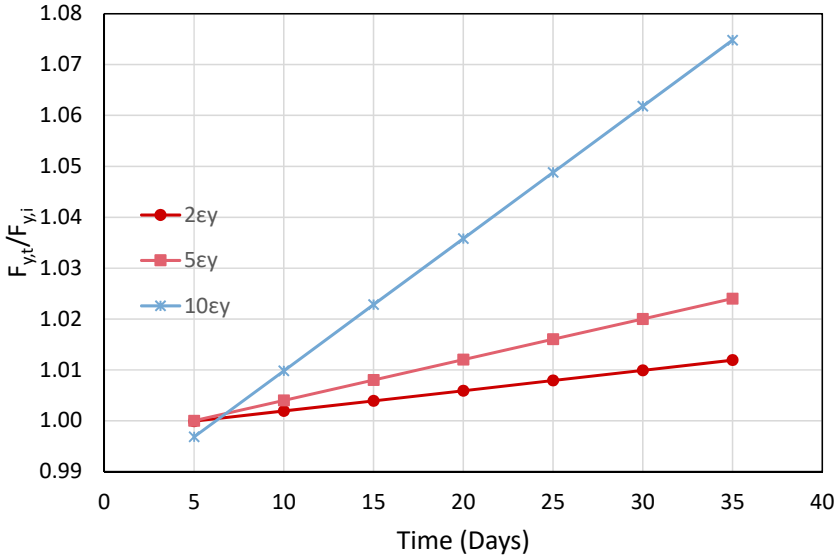

Figure 4.14 Strain Aging effect on Yield Strength vs Time (days)

For $10\varepsilon_y$

$$\frac{f_y}{f_{yi}} = 0.0026t + 0.9838 \tag{4.9}$$

For $5\varepsilon_y$

$$\frac{f_y}{f_{yi}} = 0.0008t + 0.996 \tag{4.10}$$

For $2\varepsilon_y$

$$\frac{f_y}{f_{yi}} = 0.0004t + 0.9979 \tag{4.11}$$

It is proposed to limit the increase in yield strength to the one obtained at 50 days which

was the limit of scope of the study. These equations are plotted in Fig. 4.14

4.3 Multiple Seismic Events

The evaluation of multiple seismic events is a topic that has been scarcely studied, however their effects have been felt in numerous earthquake sequences such as Chistchurch, Italy Earthquakes and more recently the Puerto Rico Earthquake. The main thought is that after a series of earthquake the structures accumulate damage and would eventually fail, this has been attempted as it was shown in Chapter 1.

For this study it has been determined that not all damage in structures are dependent on multiple events but rather their condition when an event occours as is the case for corrosion. Other damage related phenomenons such as Strain Aging depend on the loading history and are therefore dependent on the history of extreme loading events. It is therefore proposed to study corrosion on a discrete modeling of Main Shocks each independent of the other and to study the effect on Strain Aging by using a sequence of Main Shocks.

4.3.1 Earthquake Selection

For this study the NGA2 West Database of earthquake records provided by the Pacific Earthquake and Engineering Research Insitute (PEER) [1] is used. This database consists of 599 different Earthquake events that characterize theground motions on the west coast of the contiguous United States. The data was filteres to according to the following criteria:

- Earthquake sequence
- Moment Magnitude $M_w \geqslant 5$
- $PGA > 0.04$
- $PGV > 1$ cm/s
- $Vs_{30} > 100m/s$ & $Vs_{30} < 1000$ m/s
- Lowest usable frequency is less than 1Hz
- $R_{rup} < 60km$

From this data the major earthquakes found are the following, the earthquakes can be sumarized in Fig. 4.15 which show this earthquakes as moment magnitude Mw vs rupture distance (R_{rup}).

- Chi-chi
- Managua
- Livermore
- Northridge
- Duzce
- Mammoth lake

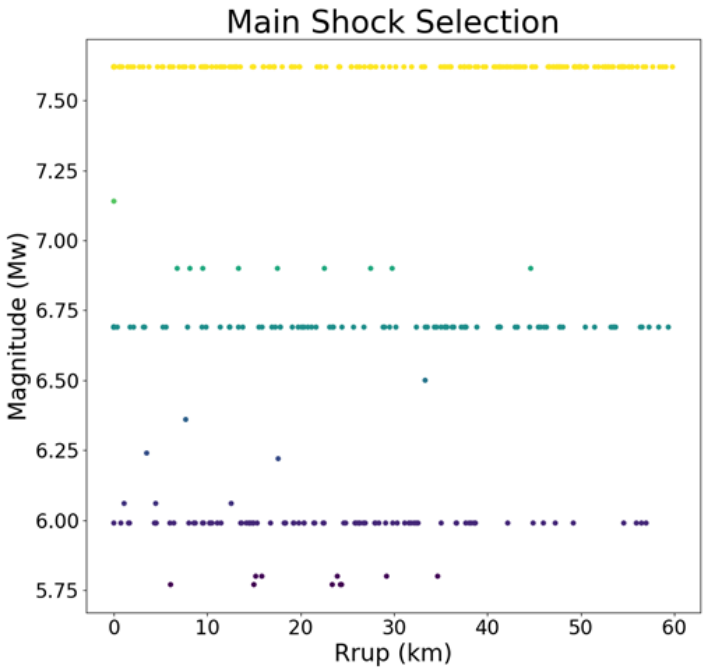

Figure 4.15 Mainshock selection from PEER NGA West2 Database

4.3.2 Discrete Modeling of Main Shock Series

The discrete modeling of mainshocks consists in using individual earthquakes that accour at different times thorughout the life of the structures which correlate to a Corrosion Level (CL), this can be done for each of the main shocks selected after which the follogin data is obtained and later analyzed:

- Maximum axial strain in Confined Concrete, Cover and Reinforcing steel Strains
- Obtain the probability of exceeding a given limit state $P(\varepsilon > \varepsilon_{LS}, IM)$
- The earthquakes are characterized according to an intensity measure

4.3.3 Multiple Main Shock Series

To simulate the life of a structure a Mainshowck series consisting of 3 Mainshocks for a the life of a structure is considered, three phases are considered:

1. at time $t = 0$ the structure has pristine conditions
2. Mainshock 1: Pristine Conditions are present. No changes to the material properties is present and no accumulation of damage has occurred.
3. Mainshock 2: Significant time after time to corrosion, mainshock 2 occours and material properties have changed due to corrosion
4. Mainshock 3: Corrosion and strain aging have occured and further modified the properties of the materials.

Similar to the discrete modeling pf main shock series the following results can be obtained:

- Maximum axial strain in Confined Concrete, Cover and Reinforcing steel Strains
- Obtain the probability of exceeding a given limit state $P(\varepsilon\varepsilon_{LS}, IM)$
- The earthquakes are characterized according to an intensity measure

4.4 Future Topics

- Concrete Strength Aging
- Welding and Fatigue in Steel Structures
- Repair Effects
- Main Shock - After Shock Series - Repair Series
- Degree of damage effect on confined structures behavior
- Selection of intensity measure (IM)

Chapter 5

Analytical Model and Preliminary Results

In this chapter first a framework for the analysis that is performed is presented, later the basic model that is used for the analysis is presented and later calibrated and verified with experimental data available in the literature. Finally preliminary results are presented that will define the general view for the proposed research

5.1 Analytical Model

5.1.1 Cantilever Column

This study focuses on the behavior of a Single Degree of Freedom (SDOF) System representing a cantilever reinforced cconcrete column. The column is modeled as shown in Fig. 5.1 This structure is modeled in OpenSeesPy [22][40] using the $forceBeamColumn$ element [30]. The forceBeamColumn element is used with two-point Gauss-Radau integration applied in the hinge regions and two-point Gauss integration applied on the element interior for a total of six integration points [30]. The force based formulation requires only a single element to accurately represent the full nonlinear deformation of the member and the integration scheme selected prevents the loss of objectivity during softening response while also providing integration points at the member ends [4],[30]. The element requires the length of plasticity be defined at each end of the member, for which the tension based rectangular plastic hinge length is calculated using the following expressions [14]:

$$L_{pc} = k * L_{eff} + 0.4D \tag{5.1}$$

$$k = 0.2 * (Fu/Fy - 1) \leqslant 0.08 \tag{5.2}$$

$$L_{pt} = L_{pc} + \gamma * D \tag{5.3}$$

For Single Bending

$$\gamma = 0.33 \tag{5.4}$$

The two-point Gauss-Radau integration is applied such that each end node integration is weighted equal to the specified plastic hinge length, as illustrated in Fig. 5.2. Therefore, strains recorded at the end sections represent accurate values even in the case where deformation localizes to the ends from strain softening behavior. For the case of the cantilever column considered, only one plastic hinge length is defined, and the opposite end is given an arbitrary unit length.

The section of the column is shown in Fig. 5.3, the section is discretized with concrete and steel material fibers. Concrete fibers are modeled using the $Concrete01$ material, modified for confined material strength based on the Mander confined concrete model [21]. The $Steel02$ material, based on the Giuffre-Menegotto-Pinto model [9] and it is used for the longitudinal reinforcement with recommended parameters ($b = 0.01, R0 = 20, cR1 = 0.925, cR2 = 0.15$).

5.1.2 Strain Penetration

The strain penetration is necessary to be considered to take into account the additional deformation due to anchorage of the reinforcement into the foundation, since the strains of tension in the reinforcement will drop to zero at a depth equal to the true development length of the rebar [27]. Experimental studies have generally reported that this end rotation contributes up to 35% to the lateral deformation of flexural members[39] and it is therefore important to incorporate into the analytical model. A way to capture this effect is by using a zero-length section element implemented in nonlinear fiber-based analysis of concrete structures, this is available in the material library of OpenSeesPy as $BondSP1$ [39] this is material model used for the steel fibers of the zero-length section element.

The required parameters for this model are:

- F_y Yield strength of the reinforcement steel
- S_y Rebar slip at member interface under yield stress (see Eq. 5.5)

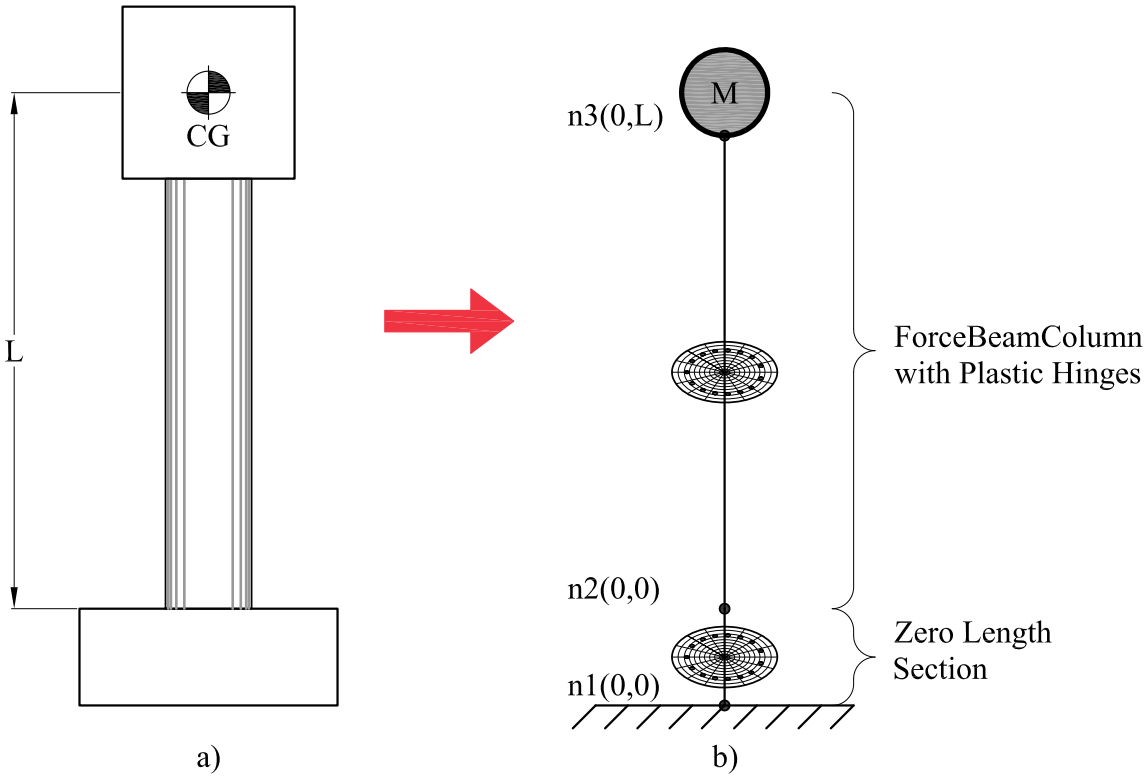

Figure 5.1 Structural Model a) SDOF Column b) Structural Model

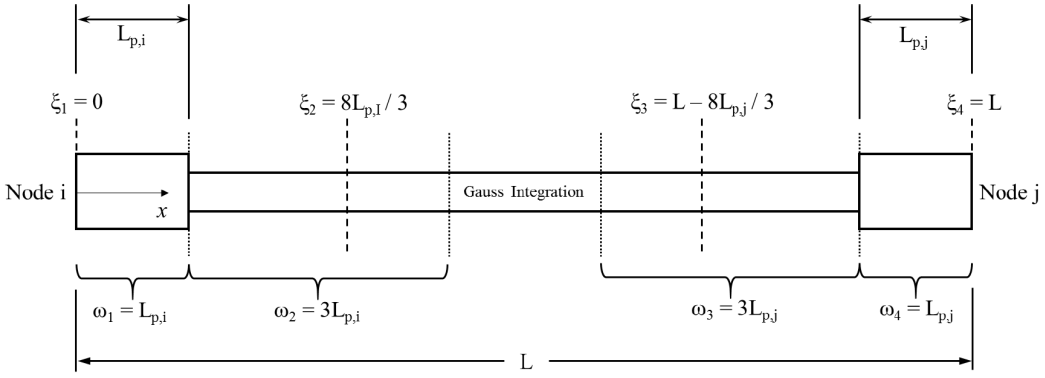

Figure 5.2 End point plastic hinge method [30]

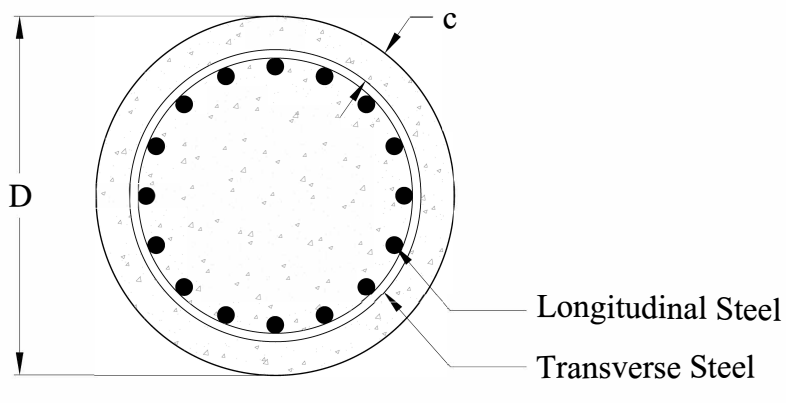

Figure 5.3 Section of the RC Column

- F_u Ultimate strength of the reinforcement steel
- S_u Rebar slip at the loaded end at the bar fracture strength a value of $35S_y$ is recommended [39]
- b Initial hardening ratio in the monotonic slip vs. bar stress response $b = 0.45$ is recommended [39]
- R Pinching factor for the cyclic slip vs. bar response $R = 1.01$ is recommended [39]
- d_b Rebar diameter
- $f'c$ Concrete compressive strength of the adjoining connection member
- α Parameter used in the local bond-slip relation and can be taken as $\alpha = 0.4$ in accordance with CEB-FIP Model Code 90 [6]

Bar slip is calculated as:

$$S_y(in) = 0.1 \left(\frac{d_b F_y}{4000\sqrt{f'_c}} (2\alpha + 1) \right)^{\frac{1}{\alpha}} + 0.013(in) \tag{5.5}$$

5.1.3 Design Limit States

Design limit states are defined on the basis of strains in the material since they can more accurately represent the different performance level of a structure. Structure limit states are

defined for tension strains in the rebars or compression strains in the concrete core. The values recommended in typical performance based design of reinforced concrete bridge columns are shown in Table 5.1. The serviceability limit states correspond to the compression strain at which concrete cover begins to crush and the peak tension strain which results in residual crack widths of approximately 1 mm. These limits are generally accepted as nominal limit states for RC members. The compression limit state for damage control is defined by the expresion shown in Eq. 5.6 and it refers to the compression strain in the confined concrete at which fracture of the transverse reinforcement confining the core occurs [27]. This equation is obtained using the strain-energy balance between that absorbed by the confined core concrete and the capacity of the confining steel. The tension damage control limit state is defined by the strain at the onset of buckling which can be expressed according to 5.7, this equation demonstrated accurate predictions of the onset of bar buckling on physical tests in SDOF Concrete Column [13]. This limit states could change as a result of the experimental campaign explained in Chapter 4.

$$\varepsilon_{c,spiralyield} = 0.009 - 0.3\frac{A_{st}}{A_g} + 3.9\frac{f_{yhe}}{E_s} \tag{5.6}$$

$$\varepsilon_{s,BB} = 0.03 + 700\rho_s\frac{f_{yhe}}{E_s} - 0.1\frac{P}{f'_c A_g} \tag{5.7}$$

Table 5.1 Design Limit States

Limit State	Concrete Limit State $\varepsilon_c(in/in)$	Reinforcing Steel Limit State $\varepsilon_s(in/in)$
Serviciability	0.004	0.015
Damage Control	Eq. 5.6	Eq. 5.7

5.2 Comparison with existing physical Tests

5.2.1 Pristine Condition Columns

The analytical model was calibrated with a tests performed by Goodnight et al [14]. These tests were performed on a SDOF cantilever column with the geomtry presented in Fig. 5.2. The parameters used in this circular column are:

- Diameter $D = 24.0inch$

- Height of the column $L = 8.0ft$
- Yield strength of steel $f_y = 574.0MPa$
- Ultimate strength of steel $f_u = 753.3 * MPa$
- Longitudinal steel volumetric ratio $\rho_s = 1.5\%$
- Transverse steel volumetric ratio $\rho_v = 1.0\%$
- Strength of concrete at 8 days $f'_c = 39.8MPa$

These parameters are used in the analytical program. The results show good agreement between the analytical model and the experimental results as shown in Fig. 5.5. This helps to assure that the results obtained from the model are reliable.

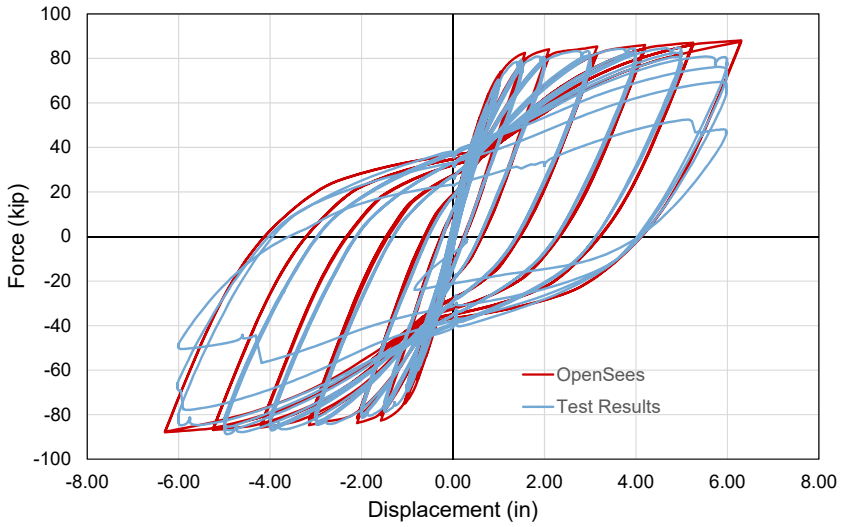

Figure 5.4 Force-Displacement results from experimental results [14] and analytical model

5.2.2 Accelerated Corrosion Columns

The results from Ma et al [19] were used to compare the test results against analytical results. The column used had the following parameters:

- Diameter $D = 260.0mm$

- Height of the column $L = 820.0ft$
- Yield strength of steel $f_y = 375.0MPa$
- Ultimate strength of steel $f_u = 572.3 * MPa$
- Longitudinal steel volumetric ratio $\rho_s = 1.5\%$
- Transverse steel volumetric ratio $\rho_v = 1.0\%$
- Strength of concrete at 8 days $f'_c = 39.8MPa$
- Corrosion level $CL = 9.5\%$

Using equation Eq. 4.7 the material properties of steel were modified accordingly. Fig. **??** show that the results obtained from the analytical model are able to capture the response of the structure before bar fracture and bar buckling occur. After this has occured the model over predicts the response.

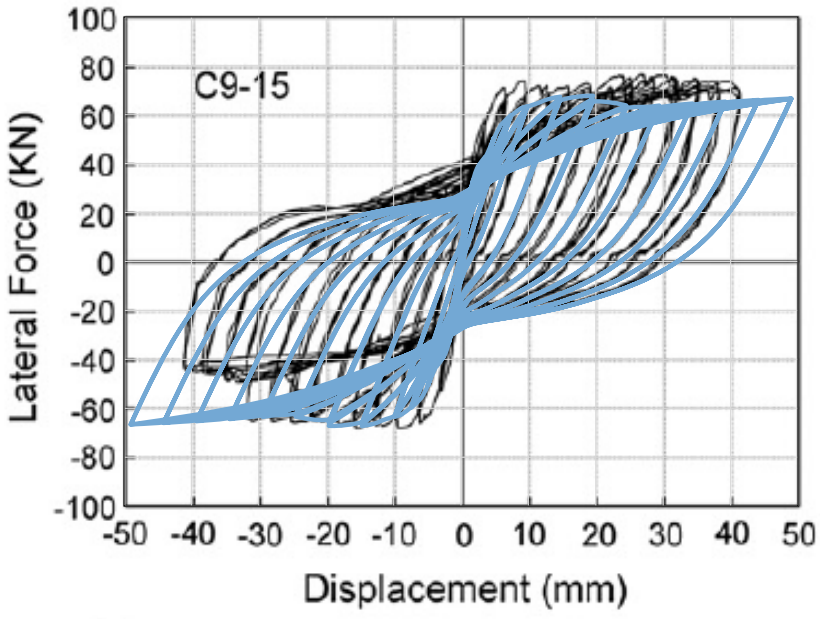

Figure 5.5 Force-Displacement results from experimental RC column with corrosion in logitudinal bar (CL=9.5%) results [19] and analytical model (shown in lightblue)

Table 5.2 Analysis Matrix

ANALYSIS MATRIX		
Description	Parameter	Range
Diameter of Column	D	30-90 in
Column Length to Diameter Ratio	L/D	8-Feb
Longitudinal Ratio	ρ_s	0.01-0.04
Transverse Volumetric Ratio	ρ_v	0.005-0.015
Axial Load Ratio	ALR	0.05-0.2
water to cement ratio	w/c	0.36-0.6
cover	c	1.5-3 in
Time/Condition	CL	5%-20%

5.3 Analytical Framework

An overall analytical framework is established such that several analysis can be performed. From this analysis it is possible to determine the effects of damage in the performance of structures. The proposed analytical framework consists in:

1. Geometrical Properties of the SDOF column
2. Properties of the material are evaluated (i.e. water to cement ratio, cover)
3. For equal periods of time the Time Dependent Properties are modified
4. Nonlinear Time History Analysis are performed for discrete events or sequence of events
5. Results are obtained and evaluated

The analytical parameters used in this study are shown in Table 5.2

5.4 Results from NLTHA

This section presents the results obtained from a non-linear time history analysis (NLTHA) performed using OpenSeesPy [40]. The structure was subjected to a total of 18 earthquake records selected from the earthquake selection showed in section 4.3.1. The main responses obtained from this analysis correspond to the maximum strains obtained for the different levels of corrosion.

The structure used for this results currently correspond to the parameters shown in section 5.2.1. The structure was analyzed for a range of corrosion level [1.5%-13%] in the longitudinal rebars.

5.4.1 Effect on structure response

As an example of the results obtained using NLTHA figures Fig. **??** and Fig. 5.7 are presented. These results are extracted from the response of the structure to the Chi-Chi earthquake. Fig. **??** Shows the global system response and Fig. 5.7 shows the stress-strain response of the extreme fiber reinforcing steel. These results show that as corrosion increases the demands imposed on the structure increases and therefore become prone to sustain more damage.

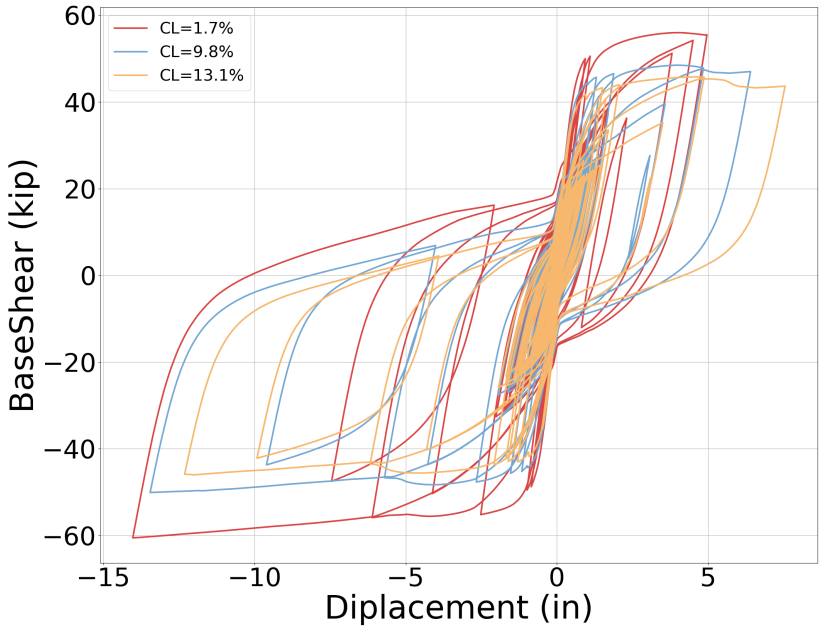

Figure 5.6 Force-Displacement results

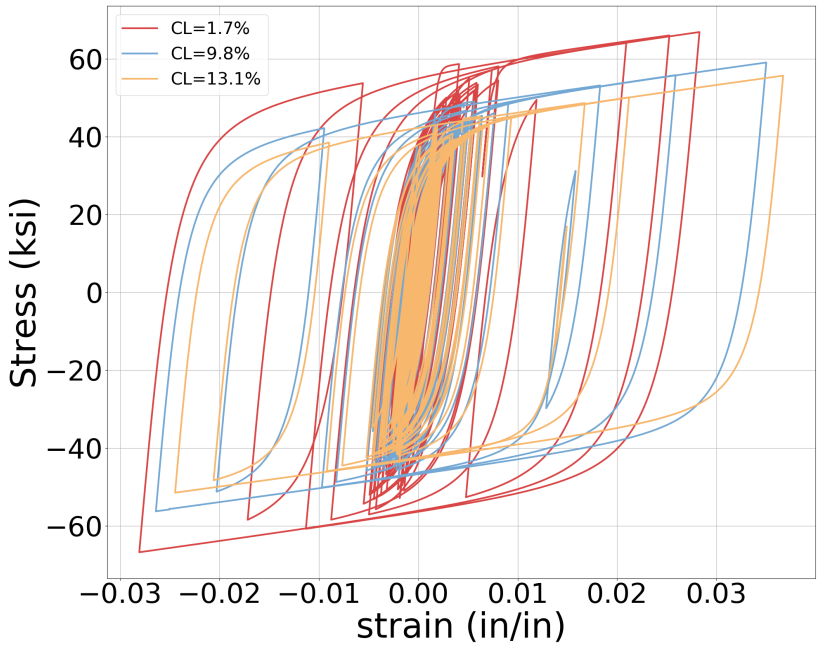

Figure 5.7 Stress strain response for extreme rebar location

5.4.2 Cumulative distribution functions

To sumarize the results obtained for all the earthquakes analyzed in this study a cumulative distribution function is used. The methodology employed corresponds to that recommended by Baker et al [2]. Figures Fig. 5.8 and Fig. 5.9 present a series of CDF graphs for steel yielding limit states as an example of the results that can be obtained from the analysis. More analysis will help improve these results. These figures however show that $IM = Sd(T_1)$ presents better correlation than those obstained by seelcting $IM = PGA$. Thus it shows that $IM = Sd(T_1)$ is a better intensity measure than $IM = PGA$ these correlates well with a recent study performed by Krish et al [17].

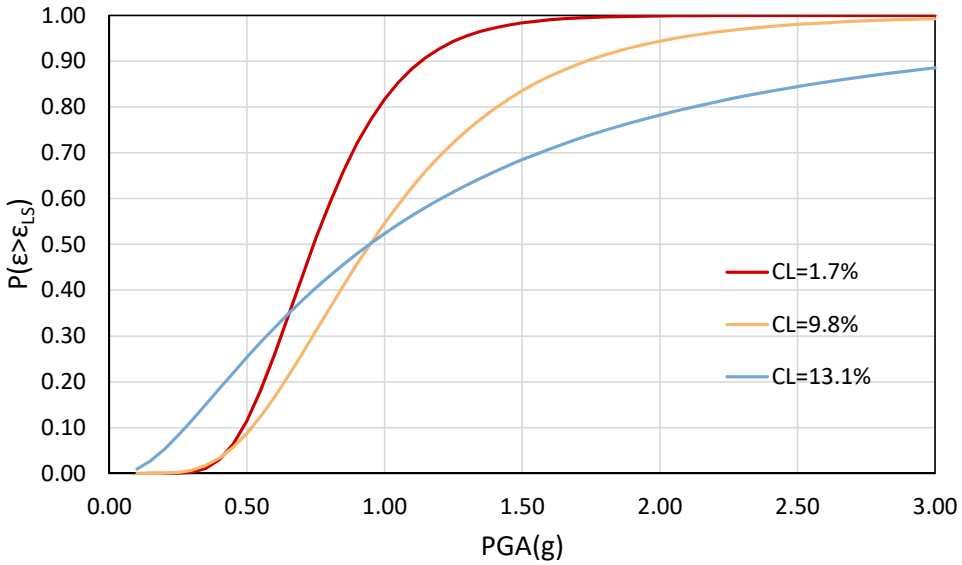

Figure 5.8 CDF of steel yielding limit state using IM=PGA

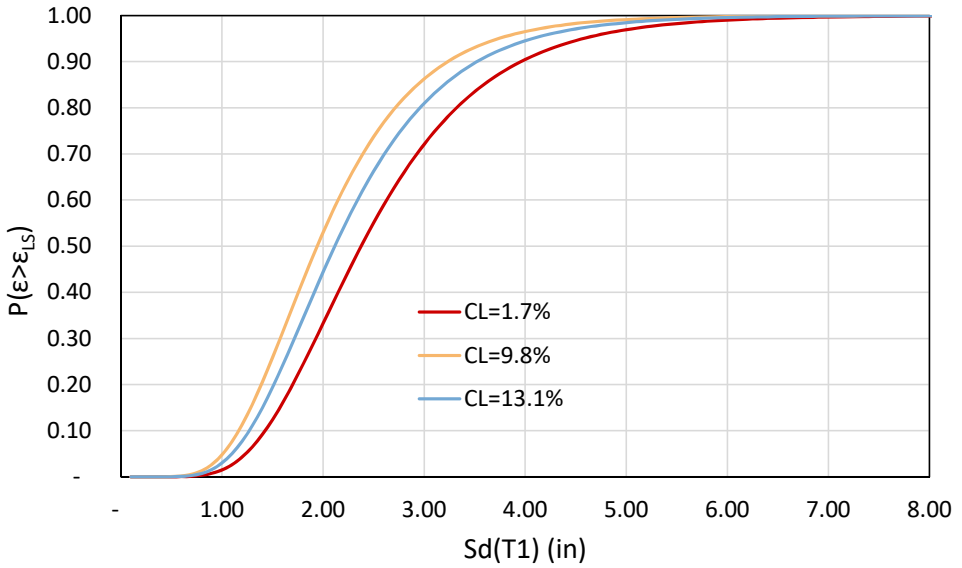

Figure 5.9 CDF of steel yielding limit state using $IM = Sd(T_1)$

5.4.3 Results discussion

- The results show that there is an increase in the demands as the corrosion in the structure increases. This is clearly shown in Fig. 5.9. However more results will help improve the correlation
- Results shown in Fig. 5.8 and Fig. 5.9, show that $IM = Sd(T_1)$ is a better inensity measure than $IM = PGA$
- The outcomes from the experimental campaign will further improve the results obtained in the analytical phase.
- The experimental phase will also provide an improved methodology to mimic the behavior of corroded reinforcing steel that is embedded inside the concrete.
- The inclusion of additional aging conditions in the analysis will provide a realistic analysis of aging RC Columns.

BIBLIOGRAPHY

[1] Ancheta, T. D., Darragh, R. B., Stewart, J. P., Seyhan, E., Silva, W. J., S-J Chiou, B., Wooddell, K. E., Graves, R. W., Kottke, A. R., Boore, D. M., Kishida, T. & Donahue, J. L., "NGA-West2 Database," 2014.

[2] Baker, J. W., "Efficient analytical fragility function fitting using dynamic structural analysis," *Earthquake Spectra*, **31**, no. 1, pp. 579–599, 2015.

[3] Barcley, L. & Kowalsky, M., "Critical Bending Strain of Reinforcing Steel and Buckled Bar Tension Test," *ACI Materials Journal*, **116**, no. 3, 2019.

[4] Calabrese, A., Almeida, J. P. & Pinho, R., "Numerical issues in distributed inelasticity modeling of rc frame elements for seismic analysis," *Journal of Earthquake Engineering*, **14**, no. sup1, pp. 38–68, 2010.

[5] Choe, D.-E., Gardoni, P., Rosowsky, D. & Haukaas, T., "Probabilistic capacity models and seismic fragility estimates for RC columns subject to corrosion," *Reliability Engineering & System Safety*, **93**, no. 3, pp. 383–393, 2008.

[6] Comité Euro-Intenational du Betón, *CEB-FIP Model Code 90*, 1st. London, 1993.

[7] Enright, M. P. & Frangopol, D. M., "Probabilistic analysis of resistance degradation of reinforced concrete bridge beams under corrosion," *Engineering Structures*, **20**, no. 11, pp. 960–971, 1998.

[8] Fajfar, P., "Equivalent ductility factors, taking into account low-cycle fatigue," *Earthquake Engineering & Structural Dynamics*, **21**, no. 10, pp. 837–848, 1992.

[9] Filippou, F. C., Popov, E. & Bertero, V., "Effects of bond deteroriation on hysteretic behavior of renforce concrete coint," Tech. Rep. August, 1983, p. 212.

[10] Ghods, P., Isgor, O. B., McRae, G. A. & Gu, G. P., "Electrochemical investigation of chloride-induced depassivation of black steel rebar under simulated service conditions," *Corrosion Science*, **52**, no. 5, pp. 1649–1659, 2010.

[11] Ghosh, J. & Padgett, J. E., "Aging Considerations in the Development of Time-Dependent Seismic Fragility Curves," *Journal of Structural Engineering*, **136**, no. 12, pp. 1497–1511, 2010.

[12] Ghosh, J., Padgett, J. E. & Sánchez-Silva, M., "Seismic Damage Accumulation in Highway Bridges in Earthquake-Prone Regions," *Earthquake Spectra*, **31**, no. 1, pp. 115–135, 2015.

[13] Goodnight, J. C., Kowalsky, M. J. & Nau, J., "Strain limit states for circular rc bridge columns," *Earthquake Spectra*, **32**, no. 3, pp. 1627–1652, 2016.

[14] Goodnight, J. C., Kowalsky, M. J. & Nau, J. M., "Effect of load history on performance limit states of circular bridge columns," *Journal of Bridge Engineering*, **18**, no. 12, pp. 1383–1396, 2013.

[15] Khashaee, P. & Eeri, M, "Damage-based Seismic Design of Structures," *Earthquake Spectra*, **21**, no. 2, pp. 371–387, 2005.

[16] Krawinkler, H., "Performance Assessment of Steel Component," *Earthquake Spectra*, **3**, no. 1, pp. 27–41, 1987.

[17] Krish, Z. F., "Rapid Repair of Reinforced Concrete Bridge Columns Subjected to Seismic Loading via Plastic Hinge Relocation," PhD thesis, North Carolina State University, 2018.

[18] Kunnath, S. K., Reinhorn, A. M. & Lobo, R. F., "IDARC Version 3.0: A Program for the Inelastic Damage Analysis of RC Structures," **818**, no. 1992, pp. 1–20, 1992.

[19] Ma, Y., Che, Y. & Gong, J., "Behavior of corrosion damaged circular reinforced concrete columns under cyclic loading," *Construction and Building Materials*, **29**, pp. 548–556, 2012.

[20] Mackie, K. R. & Stojadinović, B., "Performance-based seismic bridge design for damage and loss limit states," *Earthquake Engineering & Structural Dynamics*, **36**, no. 13, pp. 1953–1971, 2007.

[21] Mander, J. B., Priestley, M. J. N. & Park, R., "Theoretical stress‐strain model for confined concrete," *Journal of Structural Engineering*, **114**, no. 8, pp. 1804–1826, 1988.

[22] McKenna, F., Scott, M. H. & Fenves, G. L., "Nonlinear finite-element analysis software architecture using object composition," *Journal of Computing in Civil Engineering*, **24**, no. 1, pp. 95–107, 2010.

[23] Meda, A., Mostosi, S., Rinaldi, Z. & Riva, P., "Experimental evaluation of the corrosion influence on the cyclic behaviour of RC columns," *Engineering Structures*, **76**, pp. 112–123, 2014.

[24] Mehta, P. K. & Monteiro, P. J. M., *Concrete: Microstructure, Properties, and Materials*, 4th ed. McGraw Hill, 2014.

[25] Momtahan, A., Dhakal, R. P. & Rieder, A., "Effects of strain-ageing on New Zealand reinforcing steel bars," *Bulletin of the New Zealand Society for Earthquake Engineering*, **42**, no. 3, pp. 179–186, 2009.

[26] Padgett, J. E. & Desroches, R., "Bridge Functionality Relationships for Improved Seismic Risk Assessment of Transportation Networks," *Earthquake Spectra*, **23**, no. 1, pp. 115–130, 2007.

[27] Priestley, M., Calvi, G. M. & Kowalsky, M. J., *Displacement-Based Seismic Design of Structures*, 1st. Pavia, Italy: IUSS Press, 2007.

[28] Restrepo-Posada, J., Dodd, L. L., Park, R & Cooke, N, "Variables Affecting Cyclic Behavior of Reinforcing Steel," *Journal of Structural Engineering*, **120**, no. 11, pp. 3178–3196, 1994.

[29] Roufaiel, M. S. L. & Meyer, C., "ANALYTICAL MODELING OF HYSTERETIC BEHAVIOR OF R/C FRAMES," Tech. Rep.

[30] Scott, M. H. & Fenves, G. L., "Plastic Hinge Integration Methods for Force-Based Beam-Column Elements," *Journal of Structural Engineering*, **132**, no. 2, pp. 244–252, 2006.

[31] Stewart, M. G. & Rosowsky, D. V., "Time-dependent reliability of deteriorating reinforced concrete bridge decks," *Structural Safety*, **20**, no. 1, pp. 91–109, 1998.

[32] Thoft-Christensen, P., "Corrosion and Cracking of Reinforced Concrete," *Life-Cycle Performance of Deteriorating Structures: Assessment, Design and Management*, 2003, pp. 26–36.

[33] Vu, K. A. T. & Stewart, M. G., "Structural reliability of concrete bridges including improved chloride-induced corrosion models," *Structural Safety*, **22**, no. 4, pp. 313–333, 2000.

[34] Weyers, R. E., Fitch, M. G., Larsen, E. P., A1-Qadi, I. L., Chamberlin Albany, W. P., York, N. & Hoffman, P. C., "Service Life Estimates," Strategic Highway Research Program, Washington DC, Tech. Rep., 1994.

[35] Y. Liu & R. E. Weyers, "Modeling the Time to Corrosion Cracking in Chloride contaminated Reinforced Concrete Structures," *ACI Materials Journal*, **95**, no. 6, pp. 675–680, 1998.

[36] Yang, S.-Y., Song, X.-B., Jia, H.-X., Chen, X. & Liu, X.-L., "Experimental research on hysteretic behaviors of corroded reinforced concrete columns with different maximum amounts of corrosion of rebar," *Construction and Building Materials*, **121**, pp. 319–327, 2016.

[37] Young-Ji Park, B., H-S Ang, A. & Asce, F, "Mechanistic seismic damage model for reinforced concrete," *Journal of Structural Engineering*, **111**, no. 4, pp. 722–739, 1985.

[38] Yuan, Z., Fang, C., Parsaeimaram, M. & Yang, S., "Cyclic Behavior of Corroded Reinforced Concrete Bridge Piers," *Journal of Bridge Engineering*, **22**, no. 7, 2017.

[39] Zhao, J. & Sritharan, S., "Modeling of strain penetration effects in fiber-based analysis of reinforced concrete structures," *ACI Structural Journal*, **104**, no. 2, pp. 133–141, 2007. arXiv: `arXiv:1011.1669v3`.

[40] Zhu, M., McKenna, F. & Scott, M. H., "OpenSeesPy: Python library for the OpenSees finite element framework," *SoftwareX*, **7**, pp. 6–11, 2018.